Reconstruction of Intra-Bundle Fission Density Profile during a Postulated LOCA in a CANDU Reactor

Dan Ilas[1], Farzad Rahnema[2], Dumitru Serghiuta[3],*
Hisham Sarsour[4], Paul J. Turinsky[5], and Rudi Stamm'ler[6]
[1]Oak Ridge National Laboratory, [2]Georgia Institute of Technology [3], Canadian Nuclear Safety Commission, [4]Consultant, [5]North Carolina State University, [5]Studsvik Scandpower AS

Abstract

In this paper, results related to the reconstruction of intra-bundle fission density profile for a 37-pin CANDU-6 bundle with the highest enthalpy deposition during a postulated large LOCA stagnation break in a Bruce B core are presented. Bruce B is a nuclear power plant in Kincardine, Ontario, Canada, on the shores of Lake Huron with 4 CANDU reactors that are rated at about 750 MWe. The reconstruction of the fuel pin fission densities is based on steady-state, three-dimensional simulations with the Monte Carlo code MCNP for a subset of 27 out of 69 time steps during the first two seconds of the power pulse predicted for the fuel bundle at core location V13/8. Two-group cross section data libraries are generated for MCNP at each time step by the lattice depletion neutron transport code HELIOS-1.7. To include the effect of the surrounding core environment, the calculations are performed with time-dependent albedo boundary conditions inferred from a full core simulation of the transient by the nodal diffusion code NESTLE with HELIOS homogenized cross-sections.

It is found that the local peaking factor (LPF) in the outer ring varies during the transient, but never exceeds its value before the transient. Inclusion of the core environment increases the LPF in the outer ring. For the analyzed case, the increase is 0.72% with a relative error of 0.01% for the LPF before the transient and 0.55% (with a relative error of 0.01%) for the maximum *average* LPF during the transient. The latter is based on only four selected transient time points. Note that the immediate environment of the "hot bundle" does not contain any reactivity devices or other perturbing factors. As a result, the increases observed in the LPF in the outer ring may not be representative of the situations in which "other" core environment perturbing factors are present. To determine the effect of these factors on the LPF, further analyses of a bundle in the proximity of control devices should be carried out.

KEYWORDS: CANDU, pin fission density, LOCA, Monte Carlo

[*] Corresponding author: Nuclear and Radiological Engineering/Medical Physics Programs; George W. Woodruff School; Georgia Institute of Technology; Atlanta, GA, 30332-0405; Tel 404-894-3731, Fax 404-894-3733, E-mail: farzad@gatech.edu

1. INTRODUCTION

The hot pin enthalpy is a key fuel performance parameter used to assess the safety margins to acceptance criteria related to fuel and fuel channel integrity. A bounding conservative value for bundle radial peaking factor is used in safety analysis for estimating the fuel pin power distribution.

The intra-bundle power profile can be described by a pin power peaking factor hereafter referred to as the local peaking factor (LPF). Factors that affect the LPF include bundle burnup, coolant density and temperature distributions, fuel temperature distribution, and the environment of the bundle in the core, such as burnup and coolant density distributions of neighboring bundles and any reactivity devices that may be present in nearby locations (environment). A study is conducted to asses the effect of core environment on the LPF in the bundle with the highest enthalpy deposition during a postulated large break LOCA in a CANDU core. The study involves two steps. (1) Full-core simulation of a postulated large break LOCA in a Bruce B core is carried out using the nodal diffusion code NESTLE (Sarsour and Turinsky, 2003). Power pulse and two-group time-dependent fluxes and currents at the bundle interfaces with predicted maximum enthalpy are extracted for step 2 below. (2) Full bundle steady-state calculations are performed with MCNP4C (Briesmeister, 1997) at selected transient state conditions (time steps) with the corresponding time-dependent two-group albedo boundary conditions obtained from the NESTLE transient calculations.

The lattice depletion code HELIOS (Villarino, et al., 1992), version 1.7 (Simeonov, 2002) is used to generate two-group cross sections for NESTLE (Turinsky et. al., 1994) and MCNP. The NESTLE cross sections which are homogenized over the lattice cell are functions of thermal hydraulic condition. An interpolator is used to obtain the homogenized cross sections at each bundle position according to the specific local thermal hydraulic conditions during the postulated transient. The MCNP two-group library which contains pin-wise macroscopic cross-sections is generated as a function of transient time. Using time dependent albedo boundary conditions and cross sections, MCNP eigenvalue calculations are performed in the bundle to simulate the fuel pin fission density distribution during the transient (power pulse).

Since the boundary condition of the bundle is non-reflective and spatially variable during the transient, MCNP is modified to handle energy and surface segment dependent albedos. The standard version allows for reflective and vacuum boundary conditions only.

The selected bundle environment during the transient is described in Section 2. The generation of the MCNP multigroup library as a function of time is discussed in Section 3. The MCNP model and the method for estimating the two-group albedo boundary condition using NESTLE core quantities are described in section 4. Finally, the results and conclusions of this study are given in sections 5 and 6, respectively.

2. BUNDLE ENVIRONMENT

A NESTLE full core simulation of the transient predicts (Sarsour and Turinsky, 2003) that the maximum energy deposition is reached in bundle position 8 in channel V13 of the core. This bundle, a 37-element CANDU lattice, with a pitch of 28.575 cm and a length of 49.53 cm, is simulated with MCNP in the steady-state mode. No reactivity device is located in its immediate

neighborhood. The averaged burnup of the bundle is 3359.449 MWd/TU. The average burnup distribution of the surrounding bundles is shown below.

Bundle Position #7

	4317.283	
4350.862	4355.770	4235.604
	4327.847	

Bundle Position #8

	4844.069	
4774.822	**3359.449**	4862.833
	4768.867	

Bundle Position #9

	5060.250	
5109.260	2245.746	5261.658
	5182.285	

The time dependent data are based on the condition of the bundle during the postulated large LOCA in the primary heat transport system at the pump discharge. The size of the break is assumed to be 60% which has been found to maximize the fuel sheath temperature due to coolant stagnation in the channel. The insertion of all shutoff rods, except # 13 and #20, is assumed to begin at 0.6023 seconds and end (fully inserted) at 1.868 seconds after the break. The power pulse (total prompt thermal power) in the core as predicted by HELIOS/NESTLE NM is shown in Figure 1.

Figure 1: NESTLE Predicted Power Pulse in the Hot Bundle

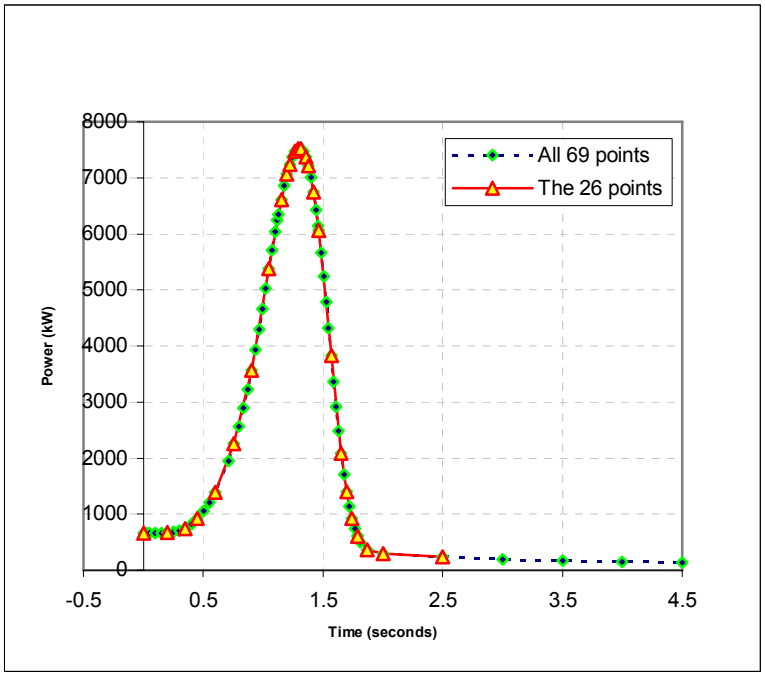

3. GENERATION OF MULTIGROUP LATTICE CELL DATA FOR MCNP

A set of 45 and 2-groupACE format cross section libraries, corresponding to the lattice cell transient states (69), is generated for the MCNP code using HELIOS. Examples of state

parameters varying with time are: fuel, gap and coolant temperatures, coolant density and bundle power density.

To reduce the large amount of cross section data generated by HELIOS for the lattice cell materials, spatial homogenization was used. Moderator, coolant and structural material (fuel clad smeared into the gap, pressure tube and calandria tube and the gap in between the tubes) are each a separate cross section material region. In collapsing the 45-group cross sections, the appropriate flux spectrum in each HELIOS spatial mesh region in these materials is used. The cross sections for the fuel materials depend not only on the state, but also on the location within the lattice cell (due to the spatial shielding calculation). As a result, two group cross sections are generated for each fuel pin in the ¼ cell HELIOS model of the bundle leading to 22 unique fuel cross section material regions Note that each fuel pin is divided into two radial regions (a thin plutonium ring and its remaining interior fuel region). The unique fuel pin material regions are color shaded in Figure 2. We note that although 45-group cross sections were generated for MCNP we only used the 2-group library for consistency with the NESTLE 2-group calculations. By contract to MCNP cross sections, the NESTLE cross sections are homogenized and collapsed over the entire cell using the 45 group HELIOS spectra as a function of time (state). Both MCNP and NESTLE libraries are transport corrected using the following transport cross section as follows.

$$\Sigma_{tc,g} = \Sigma_{ab,g} + \sum_{g'} \Sigma_{s0,g\to g'} - \Sigma_{tr,g} \qquad (1)$$

In the above equations, the subscripts "*tc*", "*ab*" and "*tr*" denote the transport correction to the total cross section, absorption and transport cross sections, respectively. The subscript *"s0"* stands for the isotropic scattering kernel.

4. MCNP MODEL AND ALBEDO BOUNDARY CONDITION CALCULATIONS

In NESTLE, the bundle is divided into 8 nodes (coarse meshes) by using $(2,1,4)$ coarse meshes in the (x,y,z) directions. Using the P_1 approximation, the NESTLE time-dependent two-group quantities (node averaged flux and the surface averaged net current and flux discontinuity factors) are used to compute the time dependent albedo on the external surface of each node. The diffusion calculations in NESTLE used a 4th order polynomial to estimate the spatial shape of the intranodal flux.

A modification is made to the MCNP code to implement the capability of modeling an albedo boundary condition for multigroup neutron problems. The albedos are defined on surface segments (*i.e.*, a sub-region of an actual MCNP surface equivalent to the external surface of each NESTLE node) and within each energy group as the ratio of the incoming to the outgoing partial currents on the surface.

$$\alpha = J_{-} / J \qquad (2)$$

Using the P_1 approximation, the partial currents are given in terms of the (heterogeneous) surface flux and the net current normal to the surface as

$$J_{\pm} \cong \Phi / 4 \pm J_n / 2 . \qquad (3)$$

Using equivalence theory, the heterogeneous surface flux is given in terms of the NESTLE homogeneous surface fluxes and discontinuity factors on the left ("–") and right (+) side of the surface as

$$\Phi = f^{+}\phi^{+} = f^{-}\phi^{-}. \quad (4)$$

The homogeneous surface fluxes are estimated from the NESTLE node average flux and the 4th order expansion coefficients for the intranodal flux shape. Therefore, use of Eqs. (3) and (4) in Eq. (2) yields the time dependent albedo boundary conditions on each surface segment of the bundle.

The angular distribution of the albedo reflection is defined on the MCNP surface card in the usual manner (*i.e.*, by preceding the surface number with a "*" for specular reflection or "+" for isotropic (white) reflection). White reflection is used in the MCNP calculations since the angular distribution of neutrons at the cell surface is expected to be nearly isotropic due to the large quantity of moderator separating the pressure tubes. The actual angular distribution at the cell boundary is not estimated from an MCNP core calculation.

Figure 3 shows an (*x,y*) cross section through the MCNP geometrical model of the bundle with the fuel pin numbering convention. Note that the moderator region is not shown in its entirety. Color shades in the fuel pins represent the fuel material distribution in the bundle. Because the material cross sections originated in a quarter lattice HELIOS model, their distribution among the pins is symmetric with respect to the (x, y) axes.

As mentioned earlier, in NESTLE, the bundle is divided into four axial nodes. For tallying purpose, the bundle in MCNP is also divided into four regions axially (z-axis). The materials are uniform along the z-axis. The outer dimensions of the parallelepiped, including the bundle, are the same as those for the bundle model in NESTLE. The MCNP library contains 2-group macroscopic cross sections for each of the two radial regions of each pin. In summary, each pin is made up of 8 geometrical regions (cells in MCNP terminology). The 2-group flux is tallied individually for each of these 8 regions in each pin (F4 type tally). As a result, 592 (=8x2x37) flux values are tallied for each time (state) point.

The MCNP flux (F4) tally for group *g* in region *i* is defined for each time point by, using standard notation,

$$\mathrm{F4}_{ig} \equiv \frac{1}{V_i} \int_{\Delta E_g} dE \int_{V_i} dV \Phi(\vec{r}, E). \quad (5)$$

In this equation, $\Sigma_f(\vec{r}, E)$ is the fission cross section at energy *E* and position $\vec{r}$, and V_i is the total volume of region *i*. Using the F4 tally values, the fission density for each pin (or each z-region within a pin) can be estimated as

$$\mathrm{FD} = \frac{1}{V} \sum_i V_i \sum_g \Sigma_{f,ig} \mathrm{F4}_{ig}. \quad (6)$$

In the above equation, $\Sigma_{f,ig}$ is the (constant) fission cross section in region *i* and group *g* and V_i is the total fuel volume. The F4 tally errors are propagated to estimate the statistical error for the fission density as

$$\sigma_{\mathrm{FD}} = \frac{1}{V} \sqrt{\sum_i \sum_g \left(V_i \Sigma_{f,ig} \sigma_{\mathrm{F4}_{ig}}\right)^2}. \quad (7)$$

The MCNP calculations use 1100 cycles of 10000 particles each. Skipping the first 100 cycles, a total of 10 million active histories are used. The fuel pin fission densities obtained from an MCNP eigenvalue calculation with specular reflection boundary conditions on all sides of the fuel bundle are taken as the infinite medium (reference) pin power distribution. To obtain the

values for the bundle in the core environment, albedo boundary conditions are used on all external faces.

MCNP estimated k-eff just prior to the initiation of the postulated event is 0.99665 ± 0.00013 for the bundle with the albedo boundary conditions inferred from the corresponding NESTLE core calculation. NESTLE predicts a core k-eff of 0.99485 for this condition. This is a difference of 1.8 mk.

Figure 2: MCNP Model – *X*-*Y* Cross Sectional View Showing Pin Numbering Convention

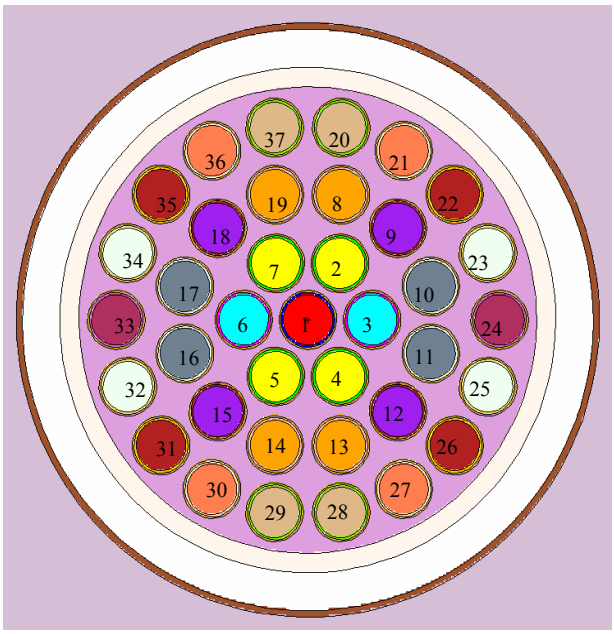

5. RESULTS

A 27 point subset of the 69 time steps is selected for the MCNP calculations. The subset covers the first 2.5 seconds of the transient. Its selection is based on ensuring that it reproduces as closely as possible the same power shape as the full set in the first 2.5 seconds. As can be seen from Figure 1, the power shape for the selected points agrees very well with that using the full set. Special attention was paid to reproduce the peak of the curve. The selected points are in bold face in Table 1.

The MCNP eigenvalue calculations are performed at each of the 27 selected time points using both an infinite medium (reference) and albedo boundary condition. The reference (full specular reflection) fission density in each fuel pin for five selected time points is plotted in Figure 3. The associated statistical uncertainties (relative errors) which are of the order of about 0.0007 are not shown in the figure. Note that the pins are numbered from the center (pin # 1) towards the periphery of the bundle. In each radial fuel ring, the numbering order is clockwise starting from the positive y axis (see Figure 2). The pin fission density values are normalized to the number of pins in the ¼ cell, so that all values are around 1.

As expected, the fission density increases from center to periphery at all times. Also, it can be seen from Figure 3 that the difference between the central pin and the pins on the outermost ring

is reduced with the increase in the coolant void fraction (from time step 0 to time 63). That is, the fission density distribution flattens as the voiding increases.

The corresponding fission density results for the albedo cases are shown in Figure 4. It can be observed that unlike the specular reflection cases, the fission density distribution in each fuel ring is not constant in the albedo cases. The largest differences are found in the outermost ring as expected. This is expected because the bundle sees the core environment through the albedo

Table 1: Power Data in Bundle V13/8 for 69 Time Steps[†]

Time Step	Time (ms)	Power (W)	Time Step	Time (ms)	Power (W)	Time Step	Time (ms)	Power (W)
0	**0.0**	**659019.7**	23	1022.9	5022242.0	46	1504.4	5238980.0
1	25.1	660807.6	**24**	**1049.7**	**5373800.0**	47	1525.1	4789850.0
2	50.2	660823.5	25	1076.1	5714584.0	48	1546.3	4316166.0
3	100.3	662310.5	26	1101.8	6034444.0	**49**	**1567.8**	**3832933.0**
4	150.4	665726.5	27	1118.6	6241698.0	50	1588.9	3365186.0
5	**200.5**	**671913.6**	28	1127.3	6345957.0	51	1609.8	2917672.0
6	250.6	683878.9	**29**	**1151.9**	**6615156.0**	52	1631.1	2485958.0
7	300.7	705220.1	30	1175.6	6855931.0	**53**	**1653.0**	**2082257.0**
8	**350.8**	**745854.7**	**31**	**1199.0**	**7067828.0**	54	1675.6	1715005.0
9	400.9	825684.1	**32**	**1222.5**	**7239853.0**	**55**	**1697.8**	**1404208.0**
10	**451.0**	**927363.4**	33	1245.5	7376859.0	56	1720.2	1141168.0
11	501.1	1057854.0	**34**	**1268.4**	**7473442.0**	**57**	**1743.2**	**921167.7**
12	551.2	1211650.0	**35**	**1290.4**	**7526590.0**	58	1766.4	745625.1
13	**601.3**	**1389788.0**	**36**	**1312.2**	**7524457.0**	59	1788.3	614961.0
14	708.8	1950880.0	37	1334.2	7475546.0	**60**	**1789.3**	**609057.5**
15	**755.4**	**2255620.0**	**38**	**1356.3**	**7373200.0**	61	1812.4	504789.8
16	797.2	2568206.0	**39**	**1378.0**	**7213530.0**	**62**	**1868.0**	**365750.3**
17	835.2	2892586.0	40	1399.0	7009322.0	**63**	**2000.0**	**297235.5**
18	870.0	3228107.0	**41**	**1420.0**	**6750768.0**	**64**	**2500.1**	**234500.9**
19	**903.1**	**3571688.0**	42	1441.3	6427841.0	65	3000.2	198489.9
20	934.8	3928154.0	43	1458.5	6140944.0	66	3500.3	171835.3
21	965.4	4294753.0	**44**	**1462.8**	**6064424.0**	67	4000.4	151358.2
22	994.9	4664782.0	45	1484.0	5658893.0	**68**	**4500.5**	**134580.1**

boundary conditions. The following observations are made regarding the local peaking factors (LPF).

1. The LPF is the highest at time 0 (the steady state case) for both the reference (1.1330 ± 0.0006) and the albedo cases (1.1411 ± 0.0006).
2. The observed variation in the LPF (over the 5 time points) is over a 2% decrease during the transient
3. The inclusion of the albedo boundary condition (core environment) increases the LPF at every time point analyzed. The increase ranged from 0.1 % to $0.8\% \pm 0.01\%$.

[†] Selected time steps are highlighted (bold characters)

Figure 3: Pin fission density distribution for the specular reflection (reference) case

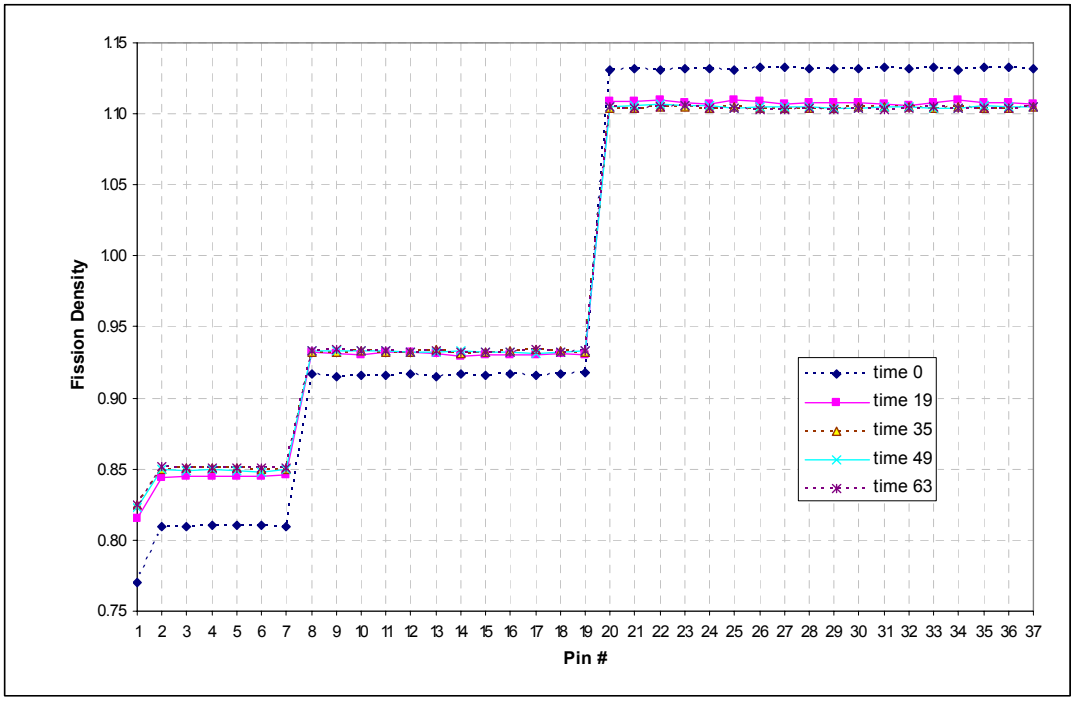

Figure 4: Pin fission densities for the albedo case

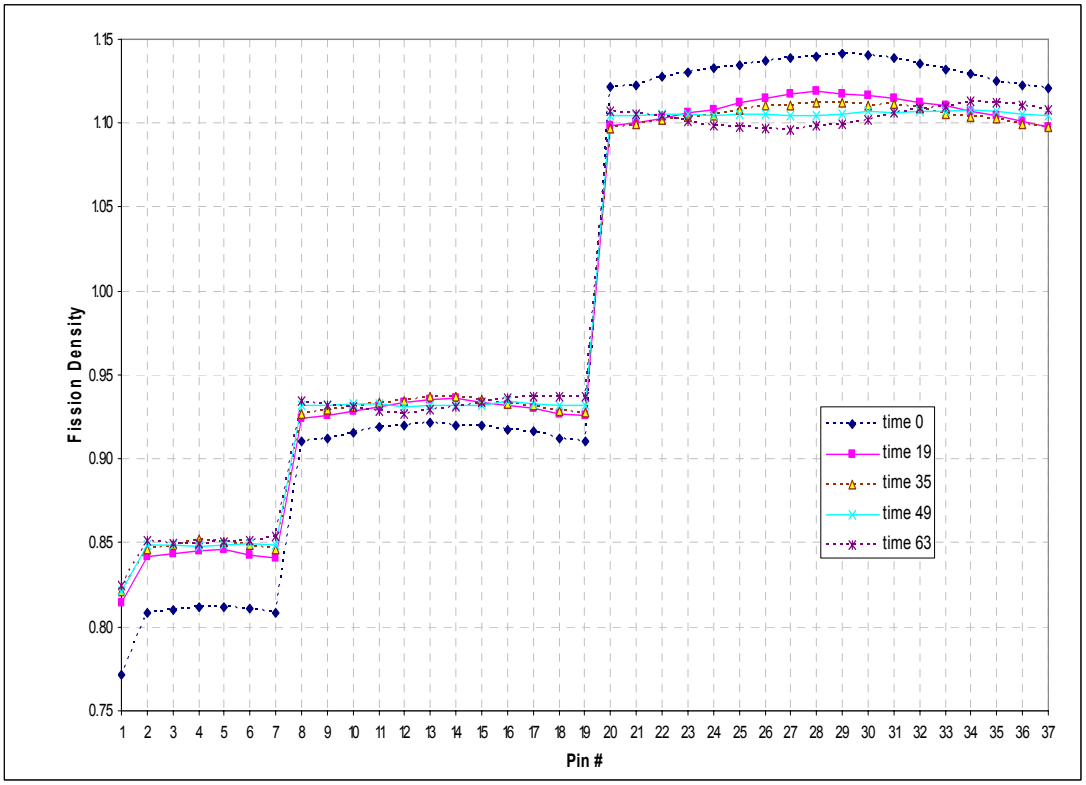

6. CONCLUSIONS AND RECOMMENDATIONS

The conclusions and recommendations of this assessment are summarized below. Note that the infinite medium results are generally used to infer the local peaking factor during a transient and the hot operating condition.

- The local peaking factor (LPF) in the outer ring varies during the transient, but never exceeds its value before the transient.
- Inclusion of the core environment increases the LPF in the outer ring. For the analyzed case, the increase is 0.72% with a relative error of 0.01% for the LPF before the transient and 0.55% (with a relative error of 0.01%) for the maximum *average* LPF during the transient. The latter is based on only four selected transient time points. Note that the immediate environment of the "hot bundle" did not contain any reactivity devices or other perturbing factors. As a result, the increases observed in the LPF in the outer ring may not be representative of the situations in which "other" core environment perturbing factors are present. To determine the effect of these factors on the LPF, further analyses of a bundle in the proximity of control devices should be carried out.
- The adequacy of using a constant value for the bundle radial form factor depends on the magnitude of the LPF in the outer ring and on the contribution of the initial stored energy to the total stored energy in the hot bundle.
- To fully address the above issue, further assessments are needed using a more refined method for pin power reconstruction from full core simulations. Further, the effect of the non-uniform pin-by-pin fuel temperature distribution needs consideration.

Acknowledgement

This work was performed as part of two research projects sponsored by the Canadian Nuclear Safety Commission (CNSC). The authors would like to acknowledge Dr. Scott Mosher for the albedo boundary condition modification of MCNP.

REFERENCES

1. Briesmeister J. F., Ed., "MCNP – A General Monte Carlo N-Particle Transport Code, Version 4B," Los Alamos National Laboratory, LA-12625-M, March (1997).
2. Ilas D. and Rahnema F., "Adequacy of Intra-Bundle Power Profile Treatment in Large LOCA Analysis," Final Report – Revision 1, NAZ-CNSC-0305R, August (2005).
3. Villarino E. A., Stamm'ler R. J. J., Ferri A. A., and Casal J. J., "HELIOS: Angularly Dependent Collision Probabilities," *Nucl. Sci. & Eng.*, **112**, 16 (1992).
4. Simeonov T. T., "Release Notes for HELIOS System 1.7," commercial Studsvik Scandpower Report, SSP-02/202, January 10 (2002).
5. Sarsour H. N. and Turinsky P. J., "Reactor Physics Aspects of LOCA Analysis: Phase 2 [CNSC Project 87055-0273], April (2003).
6. Turinsky P. J. et. al., NESTLE: A Few-Group Neutron Diffusion Equation Solver Utilizing the Nodal Expansion Method for Eigenvalue, Adjoint, Fixed-Source Steady State and Transient Problems, EGG-NRE-11406, INEL, 1994.